Central electromagnetic production of W^+W^- in proton-proton collisions

Marta Łuszczak

Department of Theoretical Physics, University of Rzeszow, Poland

4th Elba Workshop on Forward Physics and LHC Energy
25 May 2018, La Biodola, Isola d'Elba, Italy

Inclusive production of W^+W^- pairs

two different approach are possible:

- collinear - factorization
  - M. Luszczak, A. Szczurek and Ch. Royon, JHEP 1502 (2015) 098
- k_t - factorization
  - M. Luszczak, W. Schafer and A. Szczurek, Phys.Rev. D93 (2016) 074018
  - M. Luszczak, W. Schafer and A. Szczurek, JHEP 1805 (2018) 064
  - L. Forthomme, M. Luszczak, W. Schafer and A. Szczurek, arXiv:1805.07124

in collinear - factorization approach one needs photons as parton in proton:

- MRST
- NNPDF
- LUX

QED parton distributions

- **MRST-QED parton distributions**
  - QED-corrected evolution equations for the parton distributions of the proton

$$
\begin{aligned}
\frac{\partial q_i(x,\mu^2)}{\partial \log \mu^2} &= \frac{\alpha_S}{2\pi}\int_x^1 \frac{dy}{y}\left\{P_{qq}(y)\; q_i(\frac{x}{y},\mu^2) + P_{qg}(y)\; g(\frac{x}{y},\mu^2)\right\} \\
&+ \frac{\alpha}{2\pi}\int_x^1 \frac{dy}{y}\left\{\tilde{P}_{qq}(y)\; e_i^2 q_i(\frac{x}{y},\mu^2) + P_{q\gamma}(y)\; e_i^2 \gamma(\frac{x}{y},\mu^2)\right\} \\
\frac{\partial g(x,\mu^2)}{\partial \log \mu^2} &= \frac{\alpha_S}{2\pi}\int_x^1 \frac{dy}{y}\left\{P_{gq}(y)\; \sum_j q_j(\frac{x}{y},\mu^2) + P_{gg}(y)\; g(\frac{x}{y},\mu^2)\right\} \\
\frac{\partial \gamma(x,\mu^2)}{\partial \log \mu^2} &= \frac{\alpha}{2\pi}\int_x^1 \frac{dy}{y}\left\{P_{\gamma q}(y)\; \sum_j e_j^2\; q_j(\frac{x}{y},\mu^2) + P_{\gamma\gamma}(y)\; \gamma(\frac{x}{y},\mu^2)\right\}
\end{aligned}
$$

- **NNPDF2.3 parton distributions**
  - fit to deep-inelastic scattering (DIS) and Drell-Yan data

- **LUXqed17 parton distributions**
  - integral over proton structure functions $F_2(x,Q^2)$ and $F_L(x,Q^2)$

Inclusive $\gamma\gamma \to W^+W^-$ mechanism

- $\gamma\gamma$ processes contribute also to inclusive cross section

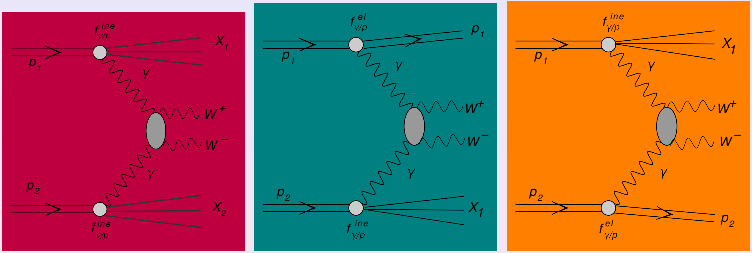

$$\frac{d\sigma^{\gamma_{in}\gamma_{in}}}{dy_1 dy_2 d^2p_t} = \frac{1}{16\pi^2 \hat{s}^2} x_1\gamma_{in}(x_1,\mu^2)\; x_2\gamma_{in}(x_2,\mu^2)\; \overline{|\mathcal{M}_{\gamma\gamma\to W^+W^-}|^2}$$

$$\frac{d\sigma^{\gamma_{el}\gamma_{in}}}{dy_1 dy_2 d^2p_t} = \frac{1}{16\pi^2 \hat{s}^2} x_1\gamma_{el}(x_1,\mu^2)\; x_2\gamma_{in}(x_2,\mu^2)\; \overline{|\mathcal{M}_{\gamma\gamma\to W^+W^-}|^2}$$

$$\frac{d\sigma^{\gamma_{in}\gamma_{el}}}{dy_1 dy_2 d^2p_t} = \frac{1}{16\pi^2 \hat{s}^2} x_1\gamma_{in}(x_1,\mu^2)\; x_2\gamma_{el}(x_2,\mu^2)\; \overline{|\mathcal{M}_{\gamma\gamma\to W^+W^-}|^2}$$

Results for MRSTQ parton distributions

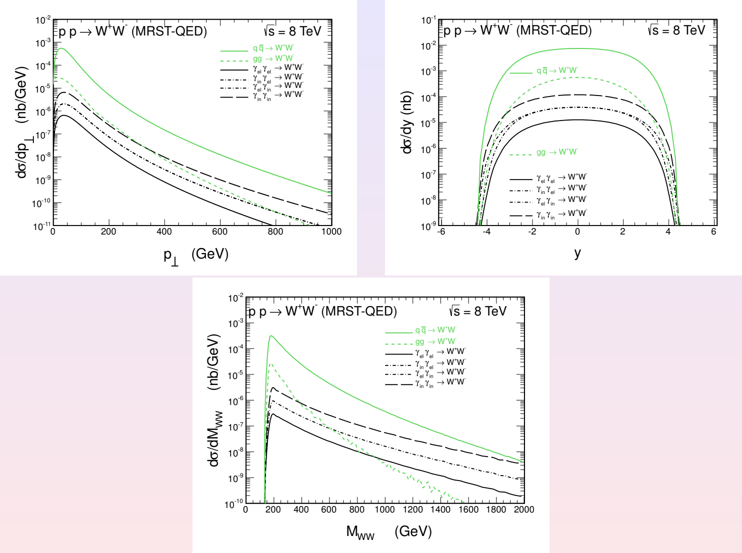

M. Luszczak, A. Szczurek and Ch. Royon, JHEP 1502 (2015) 098

Results for NNPDF2.3 QED photon distributions

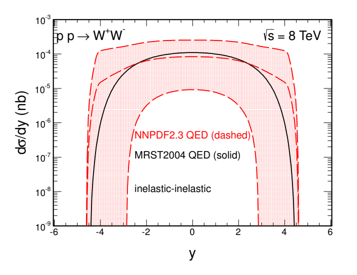

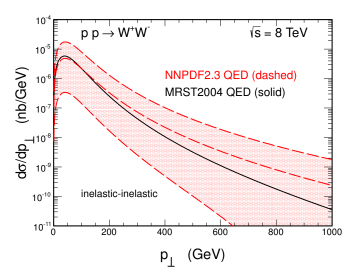

- the statistically most probable result (middle dashed line) as well as one-sigma uncertainty band (shaded area)
- very difficult to obtain the photon distributions from fits to experimental data
- limiting to both rapidities in the interval -2.5 $< y <$ 2.5 the uncertainty band becomes relatively smaller

NNPDF2.3 QED photon distributions

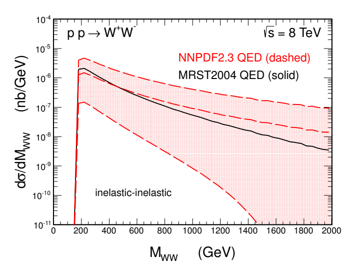

- big uncertainties can be observed especially for large *WW* invariant masses, i.e. in the region where searches for anomalous triple and quartic boson couplings are studied

M. Łuszczak, A. Szczurek and Ch. Royon, JHEP 1502 (2015) 098

Some comments on recent studies on $\gamma\gamma W^+W^-$ boson couplings

- in D0 collaboration analysis the inelastic contributions are not included when extracting limits on anomalous couplings
- the CMS collaboration requires an extra condition of no charged particles in the central pseudorapidity interval
- when comparing calculations to the experimental data the inelastic contributions are estimated by rescaling the elastic-elastic contribution by an experimental function depending on kinematical variables obtained in the analysis of the $\mu^+\mu^-$ continuum
- it is not clear whether such a procedure is consistent for W^+W^- production, where leptons come from the decays of the gauge bosons and the invariant mass and transverse momentum of the W^+W^- pair is very different than the invariant mass and transverse momentum of the corresponding dimuons

this cannot be checked in the approach with collinear photons

requires the inclusion of photon transverse momenta!

k_T-factorization approach

- the unintegrated photon fluxes can be expressed in terms of the hadronic tensor

$$\mathcal{F}^{\mathrm{in.el}}_{\gamma^* \leftarrow A}(z, \boldsymbol{q}) = \frac{\alpha_{\mathrm{em}}}{\pi} (1-z) \left(\frac{\boldsymbol{q}^2}{\boldsymbol{q}^2 + z(M_X^2 - m_A^2) + z^2 m_A^2} \right)^2 \cdot \frac{p_B^\mu p_B^\nu}{s^2} W_{\mu\nu}^{\mathrm{in,el}}(M_X^2, Q^2) dM_X^2$$

- they enter the cross section for W^+W^- production

$$\frac{d\sigma^{(i,j)}}{dy_1 dy_2 d^2\boldsymbol{p}_1 d^2\boldsymbol{p}_2} = \int \frac{d^2\boldsymbol{q}_1}{\pi \boldsymbol{q}_1^2} \frac{d^2\boldsymbol{q}_2}{\pi \boldsymbol{q}_2^2} \mathcal{F}^{(i)}_{\gamma^*/A}(x_1, \boldsymbol{q}_1) \mathcal{F}^{(j)}_{\gamma^*/B}(x_2, \boldsymbol{q}_2) \frac{d\sigma^*(p_1, p_2; \boldsymbol{q}_1, \boldsymbol{q}_2)}{dy_1 dy_2 d^2\boldsymbol{p}_1 d^2\boldsymbol{p}_2}$$

- the longitudinal momentum fractions of W^+W^- are obtained from the rapidities and transverse momenta of final state

$$x_1 = \sqrt{\frac{\boldsymbol{p}_1^2 + m_W^2}{s}} e^{y_W} + \sqrt{\frac{\boldsymbol{p}_2^2 + m_W^2}{s}} e^{y_W} ,$$

$$x_2 = \sqrt{\frac{\boldsymbol{p}_1^2 + m_W^2}{s}} e^{-y_W} + \sqrt{\frac{\boldsymbol{p}_2^2 + m_W^2}{s}} e^{-y_W}$$

Unintegrated photon fluxes from Budnev

- the quantity to compare is the differential equivalent photon spectrum

$$dn^{\mathrm{in,el}} = \frac{dz}{z}\frac{d^2\boldsymbol{q}}{\pi\boldsymbol{q}^2}\,\mathcal{F}^{\mathrm{in,el}}_{\gamma^*\leftarrow A}(z,\boldsymbol{q})$$

- for the inelastic piece

$$\begin{aligned}\mathcal{F}^{\mathrm{in}}_{\gamma^*\leftarrow A}(z,\boldsymbol{q}) \quad = \quad & \frac{\alpha_{\mathrm{em}}}{\pi}\Big\{(1-z)\Big(\frac{\boldsymbol{q}^2}{\boldsymbol{q}^2+z(M_X^2-m_A^2)+z^2m_A^2}\Big)^2\frac{F_2(x_{\mathrm{Bj}},Q^2)}{Q^2+M_X^2-m_p^2}\\ + \quad & \frac{z^2}{4x_{\mathrm{Bj}}^2}\frac{\boldsymbol{q}^2}{\boldsymbol{q}^2+z(M_X^2-m_A^2)+z^2m_A^2}\frac{2x_{\mathrm{Bj}}F_1(x_{\mathrm{Bj}},Q^2)}{Q^2+M_X^2-m_p^2}\Big\}\end{aligned}$$

- for the elastic piece

$$\begin{aligned}\mathcal{F}^{\mathrm{el}}_{\gamma^*\leftarrow A}(z,\boldsymbol{q}) \quad = \quad & \frac{\alpha_{\mathrm{em}}}{\pi}\Big\{(1-z)\,\Big(\frac{\boldsymbol{q}^2}{\boldsymbol{q}^2+z(M_X^2-m_A^2)+z^2m_A^2}\Big)^2\frac{4m_p^2G_E^2(Q^2)+Q^2G_M^2(Q^2)}{4m_p^2+Q^2}\\ + \quad & \frac{z^2}{4}\frac{\boldsymbol{q}^2}{\boldsymbol{q}^2+z(M_X^2-m_A^2)+z^2m_A^2}G_M^2(Q^2)\Big\}\end{aligned}$$

Matrix element

we obtain for the helicity-matrix element

$$
\begin{aligned}
M(\lambda_{W^+}\lambda_{W^-}) &= \frac{1}{|\vec{q}_{\perp 1}||\vec{q}_{\perp 2}|}\Big\{(\vec{q}_{\perp 1}\cdot\vec{q}_{\perp 2})\cdot\Big(\mathcal{M}(++;\lambda_{W^+}\lambda_{W^-})+\mathcal{M}(--;\lambda_{W^+}\lambda_{W^-})\Big)\\
&- i[\vec{q}_{\perp 1},\vec{q}_{\perp 2}]\Big(\mathcal{M}(++;\lambda_{W^+}\lambda_{W^-})-\mathcal{M}(--;\lambda_{W^+}\lambda_{W^-})\Big)\\
&- \Big(q^x_{\perp 1}q^x_{\perp 2}-q^y_{\perp 1}q^y_{\perp 2}\Big)\Big(\mathcal{M}(+-;\lambda_{W^+}\lambda_{W^-})+\mathcal{M}(-+;\lambda_{W^+}\lambda_{W^-})\Big)\\
&- i\Big(q^x_{\perp 1}q^y_{\perp 2}+q^y_{\perp 1}q^x_{\perp 2}\Big)\Big(\mathcal{M}(+-;\lambda_{W^+}\lambda_{W^-})-\mathcal{M}(-+;\lambda_{W^+}\lambda_{W^-})\Big)
\end{aligned} \quad (1)
$$

Results, integrated cross sections

contribution	8 TeV	13 TeV
LUX-like		
$\gamma_{el}\gamma_{in}$	0.214	0.409
$\gamma_{in}\gamma_{el}$	0.214	0.409
$\gamma_{in}\gamma_{in}$	0.478	1.090
ALLM97 F2		
$\gamma_{el}\gamma_{in}$	0.197	0.318
$\gamma_{in}\gamma_{el}$	0.197	0.318
$\gamma_{in}\gamma_{in}$	0.289	0.701
SU F2		
$\gamma_{el}\gamma_{in}$	0.192	0.420
$\gamma_{in}\gamma_{el}$	0.192	0.420
$\gamma_{in}\gamma_{in}$	0.396	0.927
LUXqed collinear		
$\gamma_{in+el}\ \gamma_{in+el}$	0.366	0.778
MRST04 QED collinear		
$\gamma_{el}\gamma_{in}$	0.171	0.341
$\gamma_{in}\gamma_{el}$	0.171	0.341
$\gamma_{in}\gamma_{in}$	0.548	0.980
Elastic- Elastic		
$\gamma_{el}\gamma_{el}$ (Budnev)	0.130	0.273
$\gamma_{el}\gamma_{el}$ (DZ)	0.124	0.267

Table: Cross sections (in *pb*) for different contributions and different F2 structure functions: LUX-like, ALLM97 and SU, compared to the relevant collinear distributions with MRST04 QED and LUXqed distributions.

Results for k_T-factorization approach

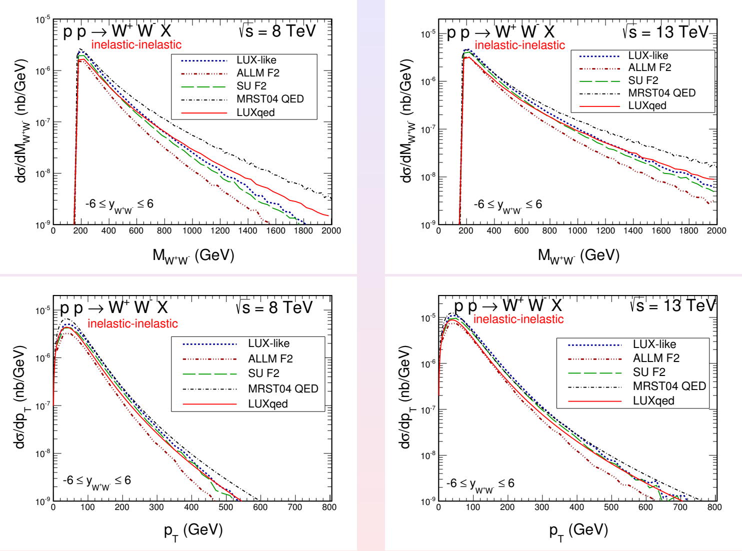

Results for k_T-factorization approach

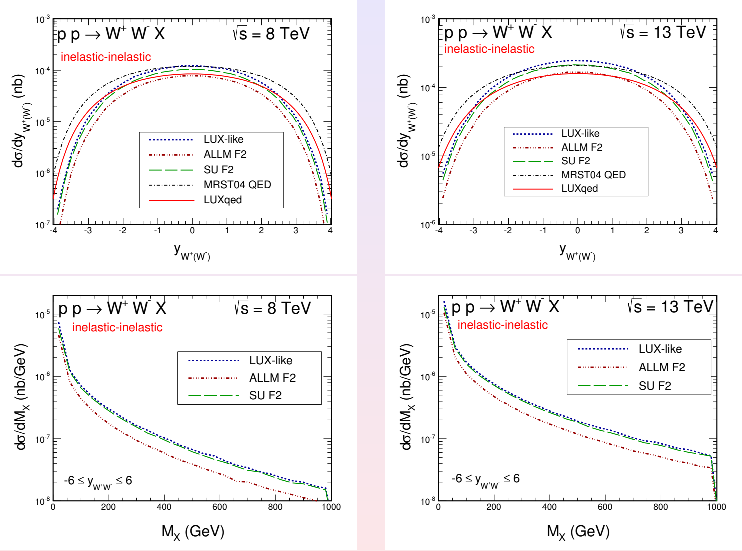

Results for k_T-factorization approach

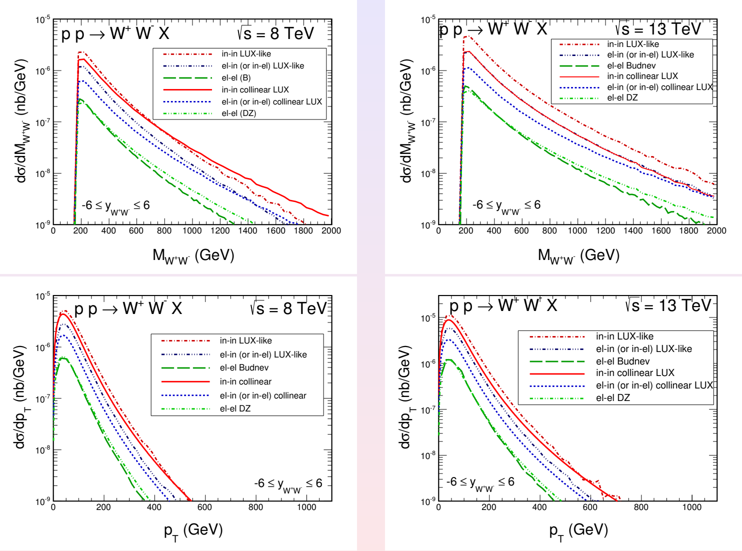

Results, correlation variables

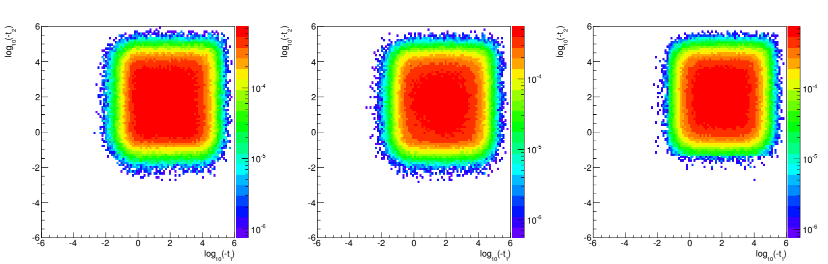

Large virtualities of photons, contradicts collinear approach

Similar pattern for different parametrizations of structure functions

Results, correlation variables

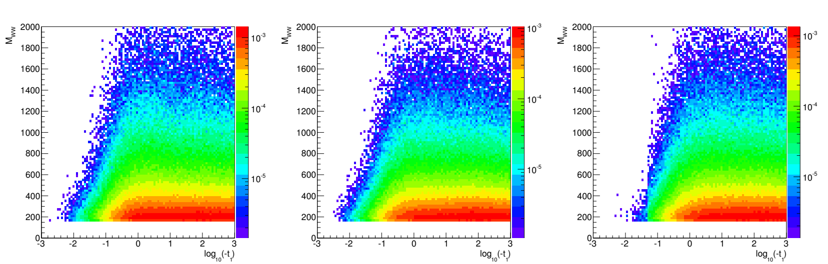

Large M_{WW} large $|t_1|$ or $|t_2|$ - strongly virtual photons

Results, correlation variables

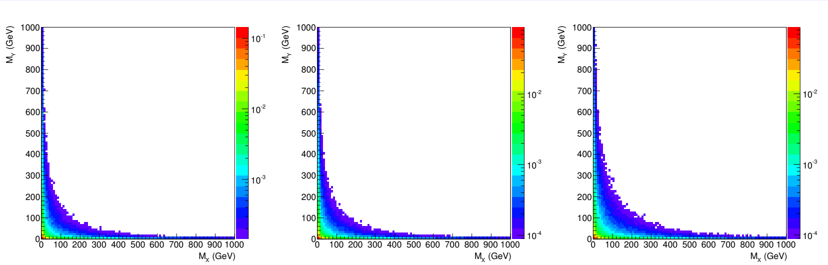

There seem to be a correlation between M_X and M_Y

When one is large, the second seems rather small

needs more attention

Results, spin decompositions

contribution	8 TeV	13 TeV
TT	0.405	0.950
LL	0.017	0.046
LT + TL	0.028 + 0.028	0.052 + 0.052
SUM	0.478	1.090

Table: Contributions of different polarizations of W bosons for the inelastic-inelastic component for the LUX-like structure function. The cross sections are given in pb.

Results, spin decompositions

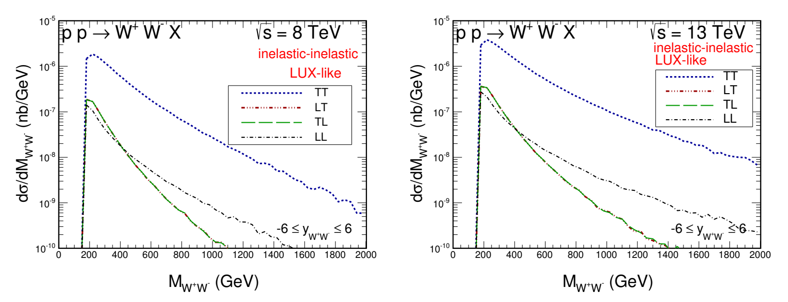

Results, longitudinal structure function

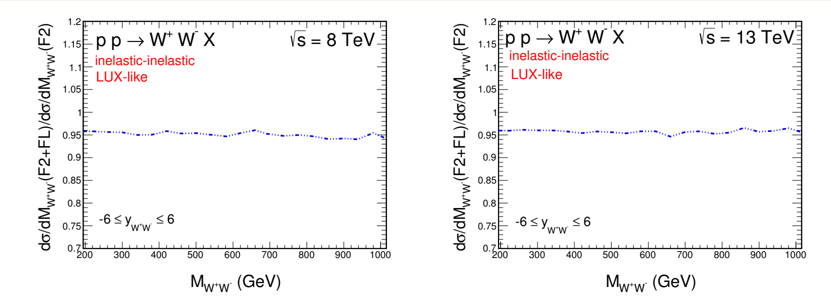

Small effect, decreasing the cross section

Results, rapidity distance between W bosons

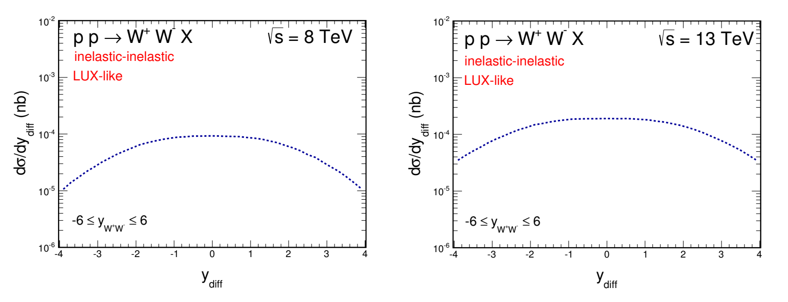

Very broad distribution

Rapidity gap survival factors caused by remnant fragmentation

- We use an implementation of the above process in CepGen for the Monte-Carlo generation of unweighted events
- The hadronisation of remnant states X and/or Y systems is performed using the Lund fragmentation algorithm implemented in Pythia8, and interfaced to CepGen. We model the incoming photon as emitted from a valence (up) quark collinear to the incoming proton direction
- Other flavour combinations are also expected to contribute to the process, but we observe the kinematics of the outgoing X and Y systems is not sensitive to this choice

Double dissociation

- distributions in pseudorapidity of particles from X ($\eta_X^{\rm ch}$) and Y ($\eta_Y^{\rm ch}$) for different ranges of masses of the centrally produced system

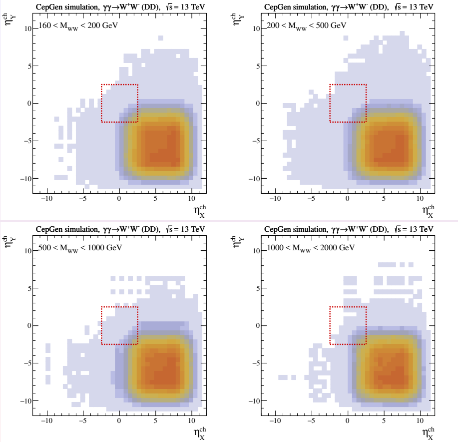

- for illustration we show by the thin square the region relevant for ATLAS and CMS pseudorapidity coverage
- the gap survival weakly depends on the invariant mass of the centrally produced

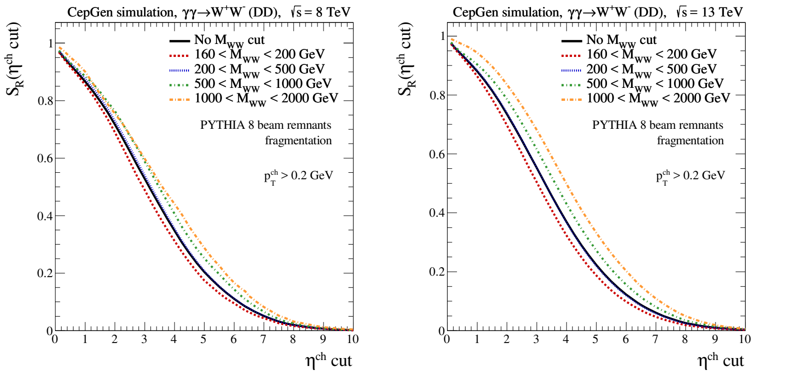

Figure: Gap survival factor as a function of the size of the pseudorapidity veto applied on charged particles emitted from proton remnants, for the diboson mass bins

- We predict a strong dependence on $\eta_{\rm cut}$. It would be valuable to perform experimental measurements with different $\eta_{\rm cut}$

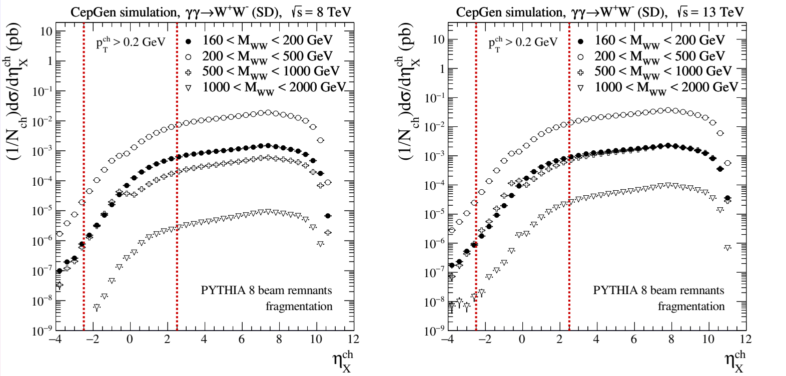

Figure: $\eta_{\rm ch}$ distribution for four different windows of M_{WW}: $(2M_W, 200\ \mathrm{GeV})$, $(200, 500\ \mathrm{GeV})$, $(500, 1000\ \mathrm{GeV})$, $(1000, 2000\ \mathrm{GeV})$. The lines show pseudorapidity coverage of ATLAS or CMS detector

- The contamination of the detector is only weakly correlated with the mass of the centrally produced system

Single dissociation

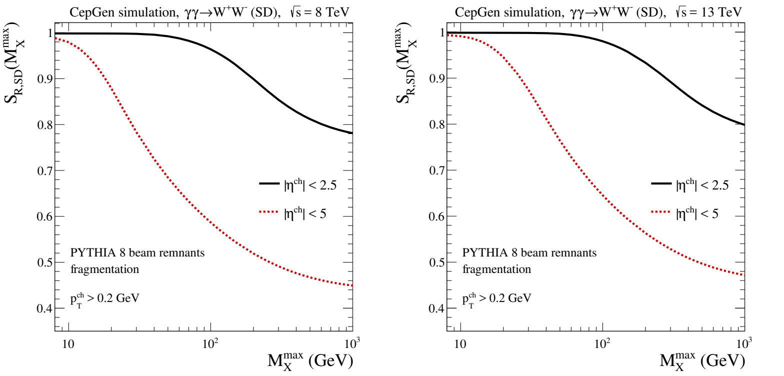

- We observe that for an $\eta_{\rm cut}$ value of 2.5 the rapidity gap survival factor S_R stays very close to 1 for $M_X^{\rm max} < 100$ GeV. Increasing the mass of the dissociative system leads to graduate destroying of the (pseudo)rapidity gap, arbitrarily fixed here to be $-2.5 < \eta < 2.5$ (ATLAS, CMS)
- The hadronisation part is independent of the system centrally produced. Hence, this method can be used to perform calculations for processes for which there are no direct procedures to perform full Monte Carlo simulations

Conclusions

- We have obtained cross section of about 1 pb for the LHC energies. This is about 2 % of the total integrated cross section dominated by the quark-antiquark annihilation and gluon-gluon fusion.
- Different combinations of the final states (elastic-elastic, elastic-inelastic, inelastic-elastic, inelastic-inelastic) have been considered.
- The unintegrated photon fluxes were calculated based on modern parametrizations of the proton structure functions from the literature.
- Several differential distributions in W boson transverse momentum and rapidity, WW invariant mass, transverse momentum of the WW pair, mass of the remnant system have been presented.
- Several correlation observables have been studied. Large contributions from the regions of large photon virtualities Q_1^2 and/or Q_2^2 have been found putting in question the reliability of leading-order collinear-factorization approach.

Conclusions

- We have presented a decomposition of the cross section into different polarizations of both W bosons. It has been shown that the TT (transversally polarized) contribution dominates and constitutes a little bit more than 80 % of the total cross section.
- The LL (both W longitudinally polarized) contribution is interesting in the context of studying WW interactions or searches beyond the Standard Model.
- We have quantifield the effect of inclusion of longitiudinal structure function into the transverse momentum dependent fluxes of photons. A rather small, approximataly M_{WW} - independent, effect was found.
- The discussed here $\gamma\gamma \to W^+W^-$ mechanism leads to rather large rapidity separations of W^+ and W^- boson
- We discussed the quantity called "remnant gap survival factor" for the $pp \to W^+W^-$ reaction initiated via photon-photon fusion